Magneto-optical study of semiconductor nanostructures in high magnetic fields

1999 J. Phys.: Condens. Matter 11 5917

(http://iopscience.iop.org/0953-8984/11/31/303)

J. Phys.: Condens. Matter **11** (1999) 5917–5928. Printed in the UK PII: S0953-8984(99)01414-9

Magneto-optical study of semiconductor nanostructures in high magnetic fields

N Miura†, Y H Matsuda, K Uchida and H Arimoto
Institute for Solid State Physics, University of Tokyo, Roppongi, Minato-ku, Tokyo, Japan

Received 29 January 1999

Abstract. A review is presented on the recent advances in magneto-optical studies of semiconductor nanostructure devices in pulsed high magnetic fields up to several hundred teslas, produced by three different techniques: electromagnetic flux compression (up to 500 T), the single-turn coil technique (up to 150 T), and non-destructive long-pulse magnets (up to 50 T). We discuss magneto-optical spectra of excitons in quantum wells, quantum wires, quantum dots, and short-period superlattices. We also discuss infrared cyclotron resonance in quantum wells under magnetic fields tilted away from the growth direction.

1. Introduction

High magnetic fields are powerful experimental tools for studying electronic states in semiconductor nanostructure devices. Excitons confined in quantum potentials exhibit quasi-two-, quasi-one- or quasi-zero-dimensional characters. Applying a magnetic field B, we can observe a magnetic field effect as the diamagnetic shift of excitons. The diamagnetic shift of excitons is generally proportional to the square of the magnetic field, B^2, and the square of the wave-function extent in the plane perpendicular to the applied field. From the coefficient of the B^2-dependence, we can obtain information on the reduced mass of excitons, and hence the binding energy. The wave-function extent of excitons confined in quantum potentials is smaller than that in three-dimensional free space, so we need high magnetic fields to observe a significant diamagnetic shift of excitons.

The relative importance of the magnetic field effect against the Coulomb energy is often represented by the so-called γ-factor, which is the ratio of the cyclotron quantization energy of the ground state to the Rydberg energy. The states of interacting electrons in high magnetic fields are characterized by this factor. The magnetic field at which γ becomes unity is $B = 2.3 \times 10^5$ T for hydrogen atoms, but for solids it is reduced to a much smaller value by a factor of m^{*2}/κ^2, where m^* is the reduced mass of the positively and negatively charged particles and κ is the dielectric constant. For $\gamma > 1$, excitonic states tend to show Landau-level-like behaviour, and the diamagnetic shift becomes a linear function of magnetic field. In very high magnetic fields, the wave-function extent of excitons becomes so small that we should be able to observe properties of excitons in the extreme high-field limit.

Besides the diamagnetic shifts of excitons, we can study the electronic states of electrons in the extreme quantum limit by measuring cyclotron resonance in high magnetic fields. The energy of the cyclotron motion becomes so large in high magnetic fields that it reaches a

† Author to whom any correspondence should be addressed.

0953-8984/99/315917+12$30.00

value comparable with the quantized energy intervals in quantum potentials or the quantum barrier height itself. When we apply high magnetic fields at an angle tilted away from the growth direction, subband–Landau-level coupling takes place. Furthermore, the final state of the cyclotron resonance transition may exceed the quantum potential barrier height in some cases. The energy levels in tilted magnetic fields exhibit complicated behaviours depending on the sample parameters and the magnetic field strength.

Recently, considerable progress has been made in techniques for measuring magneto-optical spectra in very high pulsed magnetic fields up to several hundred teslas (megagauss fields). By using streak cameras such as an image-converter camera or a CCD camera, we can obtain the entire magnetic field dependence of the spectra as continuous records with one shot of pulsed fields in the visible wavelength range. By using infrared lasers with different wavelengths and fast detectors, precision measurements of cyclotron resonance have also become possible in the megagauss range. In this paper, we present recently obtained results of high-field magneto-optical spectroscopy in both the visible and infrared wavelength ranges for nanostructure devices.

2. Experimental procedure

Pulsed high magnetic fields were produced by three different techniques: electromagnetic flux compression, which can produce fields up to 600 T, the single-turn coil technique, by which we can obtain fields up to 150 T in a bore of 10 mm diameter, and using the conventional type of non-destructive magnets for long-pulse fields up to 50 T. The waveforms of the magnetic field and the primary current of the electromagnetic flux compression are shown in figure 1.

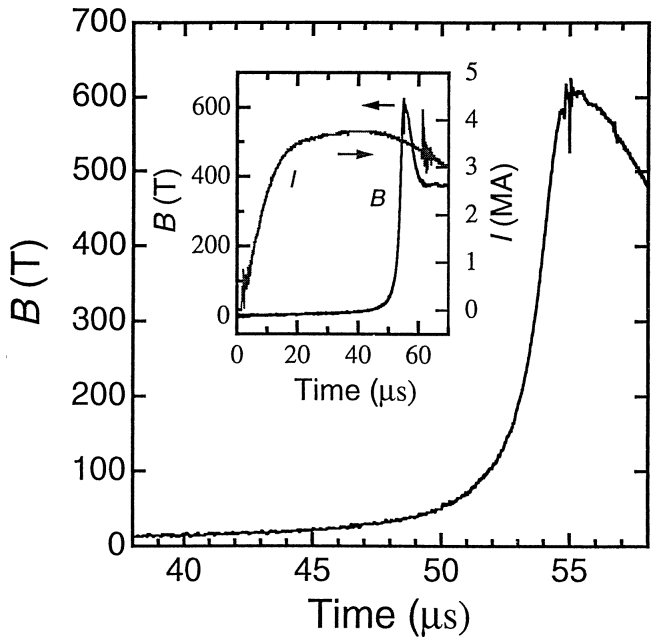

Figure 1. Profiles of the magnetic field B produced by electromagnetic flux compression. The inset shows the waveforms of the magnetic field B and the primary current I on a wider timescale.

As can be seen, the rise time of the field up to the peak in the megagauss range (>100 T) is several μs. The duration of the magnetic field pulse produced by the single-turn coil technique is also of the same order, about 7 μs [1]. Therefore, we need very fast measuring techniques in the megagauss range. In contrast, the duration of the magnetic field up to 50 T produced by non-destructive magnets is much longer (typically 15 ms), so it is useful to perform more precise measurements.

To refrigerate samples in the non-destructive fields, we use an ordinary liquid helium cryostat in which samples are immersed in liquid helium. In the megagauss fields, we use specially designed helium-flow-type cryostats made completely from plastics. The cryostat is made from phenolic tubes which are glued with Stycast glue. The sample is cooled by a liquid helium flow back and forth through the gaps between the tubes. The outside of the tubes is kept in vacuum. The sample is mounted in the innermost tube. Near the sample, a thermocouple of AuFe–chromel is set to measure the temperature. The temperature is controlled by changing the amount of helium flow. The lowest temperature that can be obtained is about 7–10 K.

For magneto-optical measurements in non-destructive long-pulse fields, we use an optical multi-channel analyser (OMA). The model OMA-IV of EG&G allows the data acquisition for streak spectra containing the full information on the magnetic field dependence of the spectra to be performed in a one-pulse shot. The main part comprises a CCD (charge-coupled device) with 512 $\times$ 512 pixels. The image of the spectra is focused on the first line of the CCD device, masking the other lines. Here the horizontal axis corresponds to the wavelength. The signals detected on the first line are transferred to the lower lines successively, utilizing the shift-register function of the CCD, while the first line keeps receiving new signals. Thus, as the time proceeds, we obtain the time-resolved spectra. When the light intensity is not sufficient for time-resolved recording, we omit the masking on the CCD frame and input the optical spectrum image on the full frame and open the gate for the input at the top flat part of the magnetic field. In this case, all 512 lines are used for the recording, so we obtain much larger sensitivity than with the streak mode. For photoluminescence (PL) measurements, the 514.5 nm line from an Ar laser was used as a radiation source, and a Xe flash lamp was used for magneto-absorption measurements.

In μs pulse magnetic fields in the megagauss range, we use an image-converter camera (Hadland Photonics Company, Model 792 with a specially large cathode) for measuring magneto-optical spectra, because it allows a much faster sweep of the optical image. The optical spectrum from the sample dispersed by a monochromator is focused on the photo-cathode of an image-converter tube. Photoelectrons are emitted from the photo-cathode in proportion to the intensity of the image. Then the electron beam is accelerated by electrodes and focused by an electric lens on the phosphor screen so that the optical image is reproduced on the screen. During this process, the electron beam is swept by a voltage ramp applied to a pair of electrodes. Thus the image of the optical spectra is streaked in the direction perpendicular to the optical spectra. As the image-converter camera itself has an image-intensifying function, and the image on the phosphor screen is further intensified by an additional image intensifier by a factor of 50–100, the spectra can be recorded with sufficiently high sensitivity in spite of the short time.

For cyclotron resonance experiments, molecular gas lasers were employed: a CO_2 laser for wavelengths (λ) of 9–11 μm, a CO laser for 5–6 μm, a pulsed H_2O laser for 16.9–119 μm, and a CO_2 laser-pumped molecular gas laser for $\lambda = 119$ μm. Fast infrared detectors were used to detect the cyclotron resonance absorption. They are a HgCdTe photovoltaic detector for $\lambda = 5$–11 μm and an extrinsic photoconducting Ge(Cu) detector for $\lambda = 16.9$ μm.

3. Results and discussion

3.1. Quasi-two-dimensional excitons of GaAs/AlAs quantum wells in very high magnetic fields

The energy states of a hydrogen atom in high magnetic fields have attracted much interest for many years as a fundamental problem of quantum mechanics. In quantum wells (QWs), we can study the properties of two-dimensional (2D) or quasi-2D excitons [2, 3]. For $\gamma > 1$, the energy shift of excitons is almost parallel to that for inter-Landau-level transitions, and the energy is expressed as

$$\mathcal{E} = \mathcal{E}_g + (N + \tfrac{1}{2})\hbar\omega_c + \mathcal{E}_{NM\lambda}$$

where N, M, and λ are the quantum numbers representing the Landau quantization, the angular momentum, and the effect of the Coulombic binding energy of electrons and holes, respectively. In high magnetic fields, the exciton wave-function extent is decreased not only in the plane perpendicular to the magnetic field but also in the direction parallel to the field. At $B = 450$ T, γ reaches 55 and the Bohr radius in the parallel direction $a_\parallel$ is reduced to about 37% of the zero-field value [4]. When we apply high magnetic fields to QWs in the direction perpendicular to the well layers, $a_\parallel$ may become less than the well width and the exciton confinement becomes ineffective. Hence a 2D-to-3D transition may show up in the quantity $\mathcal{E}_{NM\lambda}$.

We measured the magneto-absorption (MA) spectra in very high fields up to about 450 T using an image-converter camera. Figure 2 shows the MA spectra in multi-QWs with GaAs/AlAs layer thicknesses of 9 nm/5 nm for two circular polarizations, σ^+ and σ^-. At a first glance, the spectra look very complicated. For both polarizations, we can identify absorption lines corresponding to excitons, inter-Landau-level transitions, and those in higher subbands. Some lines increase their intensity with increasing field. Moreover, new lines appear in the high-field region, whereas some lines disappear in the low-energy region. It should be noted that some anomaly is visible at about 250 T on the lowest-energy line for the σ^+-polarization, and that this field is approximately equal to the field where the exciton wave-function extent in the field direction becomes comparable with the well width. The magnetic field dependences of the absorption lines exhibit complicated behaviours, which originate partly from the complicated Landau-level structure of the valence band. We calculated the valence band energies by using Ando's formulation [5]. Reasonably good agreement was obtained for the observed absorption lines.

3.2. Magneto-photoluminescence in GaP/AlP short-period superlattices and quantum wells

In short-period superlattices (SLs) of the $(GaP)_m(AlP)_n$ system (m and n are the monolayer numbers of each layer), the wave-functions of the conduction band minima are predominantly located in the AlP layer with X-point character, while those of the valence band maxima are in the GaP layer with Γ-point character. Yet the SLs show unusually intense photoluminescence of excitons, in spite of the indirect nature of the transition type both in k-space and in real space. There has been controversy concerning the mechanism of the emission. We have measured the magneto-photoluminescence (MPL) spectra of excitons in short-period SLs and QWs. When we applied magnetic fields to short-period SLs in the growth direction, we found that the intensity of the PL from excitons drastically decreased, and the peak showed a large red-shift. In contrast, when the magnetic field direction is perpendicular to the growth direction, neither the intensity nor the peak photon energy showed a significant change. In short-period SLs with $m + n =$ even number, the X point in the Brillouin zone is folded back to the Γ point, so the

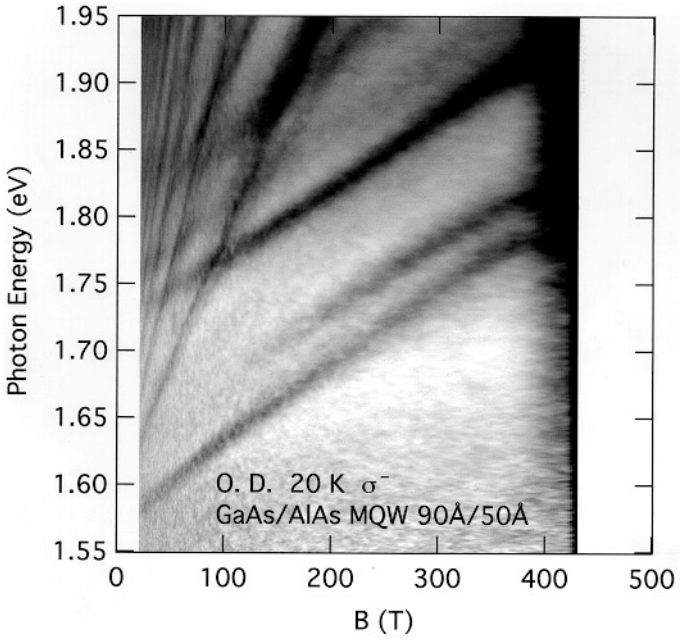

(a)

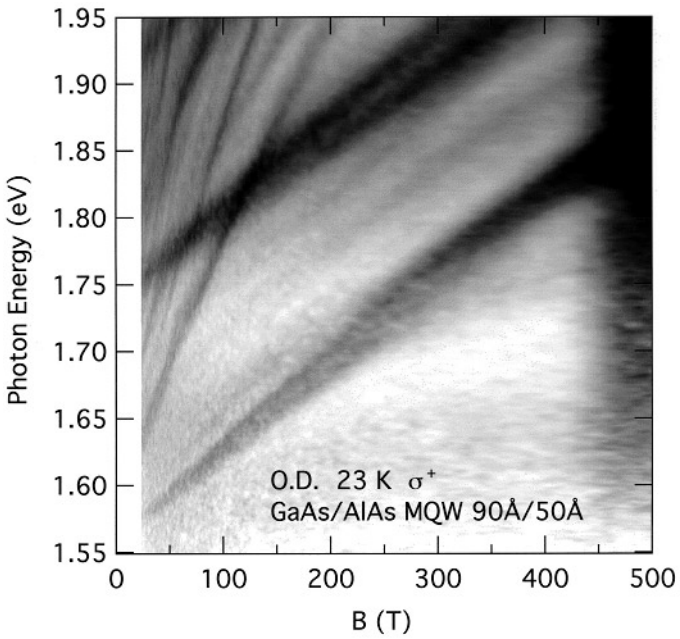

(b)

Figure 2. Magneto-absorption spectra in a GaAs/AlAs 9 nm/5 nm multi-QWs for (a) right circular (σ^+) and (b) left circular (σ^-) polarizations up to 450 T, recorded by an image-converter camera. The temperature is indicated in each frame.

transition type may become pseudo-direct. This may be considered as a reason for the strong intensity of the exciton transition [6].

We have measured photoluminescence spectra for a neighbouring confinement structure (NCS), where single layers of GaP and AlP are grown adjacently [7]. The monolayer thicknesses were 1.0 nm for both layers. The band folding does not occur in such a structure. The MPL spectra are shown in figure 3. It can be clearly seen that for $\boldsymbol{B} \perp$ layer ($\boldsymbol{B} \parallel$ growth direction), the exciton peak intensity shows a dramatic decrease and the peak shows a red-shift as shown in figure 4, while for $\boldsymbol{B} \parallel$ layer, the peak shows no such significant change. This tendency is very similar to the case for short-period SLs, and is considered to be a common

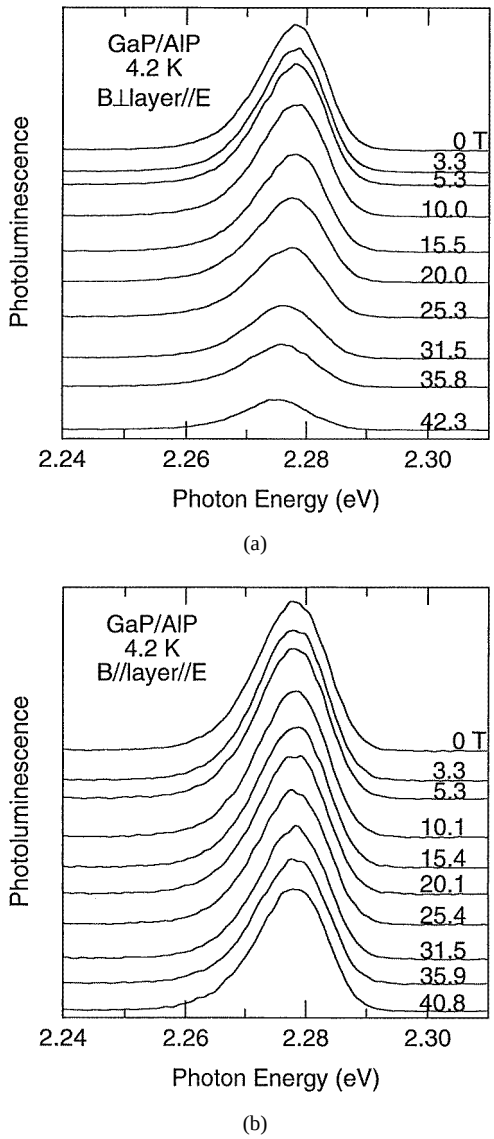

Figure 3. Magneto-photoluminescence spectra in a 1.0 nm/1.0 nm GaP/AlP NCS structure in high magnetic fields. (a) $\boldsymbol{B} \parallel$ growth direction and (b) $\boldsymbol{B} \parallel$ layers.

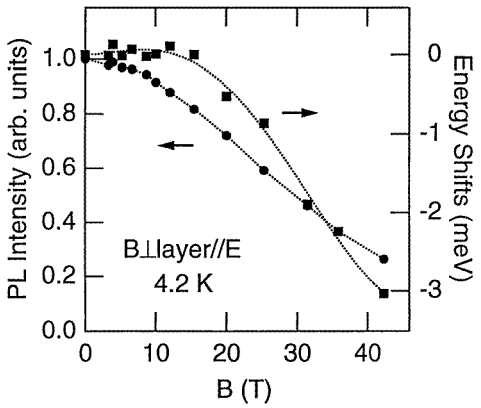

Figure 4. The photon energy and the intensity of the absorption peaks as functions of the magnetic fields in a GaP/AlP structure. The magnetic field is parallel to the growth direction.

feature of GaP/AlP structures. The present result indicates that the interface between the GaP and AlP layers plays an important role in the intense photoluminescence. Probably electrons or holes are more easily trapped in the potential minima at the interface, as the wave-function extent in the layer shrinks in high magnetic fields perpendicular to the layers [8].

3.3. Diamagnetic shifts in quantum wires

In quantum wires (QWRs), a significant anisotropy of the exciton diamagnetic shift is observed [9]. Recently, Nakashima *et al* grew QWRs with rhombic cross-sections by MBE at giant steps on a vicinal GaAs(110) surface slightly tilted towards the (110) direction [10]. QWRs of GaAs with a shape as shown in the inset of figure 5 are formed, embedded in AlGaAs barrier layers. The advantage of this technique is that a large density of QWR arrays is obtained in a layer, and, moreover, we can stack wires in accumulated layers. In such a structure, we can expect some effects of couplings between QWRs. By varying the thicknesses of GaAs and AlGaAs layers, we can change the size of the QWRs and the coupling between them. We measured MPL spectra on samples with such a structure in a long-pulse field. We observed the PL peaks from the GaAs/AlGaAs multi-QWs grown as the substrate, and from the QWRs. Figure 5 shows the PL peak energy of the two peaks for a sample with the GaAs/AlGaAs layer thicknesses of 3 nm/10 nm and 1 nm/3 nm (open circles). The well width of the QWs is large enough (30 nm) that the diamagnetic shift is almost like that for bulk GaAs, showing a very small anisotropy. On the other hand, it is evident that there is a large anisotropy in the QWR line. Reflecting the shape of the QWRs, the diamagnetic shift is largest when the field is perpendicular to the layers, and smallest for the field parallel to the QWRs. Comparing the shift with that of a sample with a smaller wire thickness (1 nm/3 nm structure), we find that shift is smaller for the thinner QWRs.

From TEM photographs for the 3 nm/10 nm sample, it was found that the rhombic cross-section has a side length of 27 nm parallel to the layer and a thickness of 9 nm. It should be noted that above 10 T, the diamagnetic shift of for the QWR is almost parallel to that of the QWs. This result is reasonable if we consider the fact that the cyclotron orbit diameter $2(\hbar/eB)^{1/2}$ is reduced to 16 nm, which is considerably smaller than the width of the QWR. From the diamagnetic shift in the region of relatively low field, we estimated the binding energy $\mathcal{E}_B$ and the Bohr radius a_B for the 1 nm/1 nm, 1 nm/2 nm, and 1 nm/3 nm samples. The binding

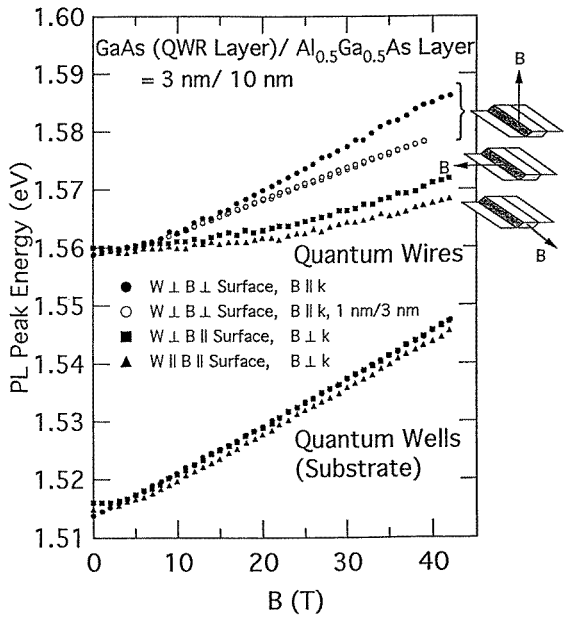

Figure 5. Magneto-photoluminescence spectra in GaAs/AlGaAs quantum wires fabricated on a vicinal GaAs surface. The layer thicknesses of the GaAs/AlGaAs layers are 3 nm/10 nm except for those shown by open circles which indicate the data for 1 nm/3 nm structure. $\boldsymbol{W}$ indicates the direction of the QWRs and $\boldsymbol{k}$ is the direction of the light propagation.

energy ranges near $\mathcal{E}_B = 8$–9 meV. The Bohr radius was found to be $a_B \sim 2$ nm along the QWR, ∼8 nm perpendicular to the QWR and parallel to the layer, and ∼10 nm perpendicular to the QWR and perpendicular to the layer. These values demonstrate a strong confinement effect in the QWRs.

Another interesting result is the barrier thickness dependence of the diamagnetic shift, because the effect of the coupling may show up. It was found for 1 nm/1 nm, 1 nm/2 nm, and 1 nm/3 nm samples that, as the layer thickness is increased, the energy of the PL peak is increased and the diamagnetic shift becomes smaller. In addition, comparing the diamagnetic shifts for two samples with different stacked layer numbers, we found that it is larger for a sample with thirty layers than for one with five layers. These results clearly demonstrate a coupling among the QWRs and the formation of a mini-band.

3.4. Magneto-photoluminescence spectra for quantum dots

In quantum dots (QDs), wave-functions of electrons and holes are confined in the quantum potential in all three dimensions. The magnetic field effect is observed as a shift or splitting of the quantized levels in the potential. The self-assembled QDs produced by Stranski–Krastanov growth realized a formation of very small dots, of size of the order of several nm. Measurements of the MPL spectra have been performed in pulsed high fields for many different kinds of QD: InAlAs/AlGaAs QDs [11], InP/GaInP QDs [12], InAs/GaAs and InGaAs/GaAs QDs [13], and InGaAs parabolic QDs [14]. For all of these samples, significant confinement effects were observed.

The Fujitsu group recently fabricated quantum dots in a tetrahedron-shaped recess (TSR) by MOVPE, utilizing the directional preference of the crystal growth [15]. The TSRs are

formed on a (111)B GaAs substrate by anisotropic etching with a mask, and comprise threefold (111)A facets. On growing an InGaAs layer (with an In composition of about 0.2) in the TSRs, QDs are formed at the bottom of the TSRs as a region where the In composition is larger than in the surrounding InGaAs layer. We measured the MPL spectra for these samples [16].

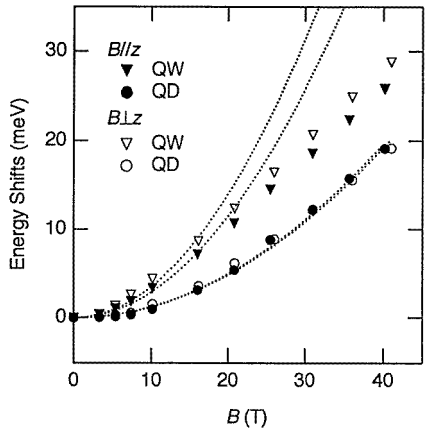

Figure 6. The magneto-photoluminescence photon energy as a function of B in InGaAs/GaAs quantum dots fabricated in TSRs. The InGaAs well thickness is 5 nm, and the height of the dot structure is 15 nm.

Figure 6 shows a typical example of the diamagnetic shift of excitons in the TSR QDs and the surrounding InGaAs QWs for a sample with the InGaAs layer thickness of $d = 5$ nm. The vertical height of the QDs is about $3d = 15$ nm. The diamagnetic shift is significantly smaller for a QD than for a QW. Furthermore, with increasing magnetic field, the peak intensity increases remarkably for a QW, whilst it decreases for a QD. We find that the anisotropy of the diamagnetic shift is not so large, reflecting the complicated shape of QDs and the fact that the directions of the InGaAs layers are oblique to the growth direction. From the diamagnetic shift proportional to B^2 in the region of relatively low field, we can estimate the 3D exciton Bohr radius of the QDs in the directions parallel and perpendicular to the growth directions as 5.7 nm and 5.8 nm. The magnetic field effect is somewhat different in samples with different structures or compositions.

3.5. The effect of tilted magnetic fields on the cyclotron resonance of GaAs/AlGaAs quantum wells

When we apply magnetic fields to 2D electrons in quantum wells tilted away from the growth direction by an angle θ, the resonant magnetic field $B(\theta)$ of the cyclotron resonance (CR) shifts to higher magnetic fields, obeying the $1/\cos\theta$ law. However, when the Landau-level spacing $\overline{h}\omega_c$ becomes large in high magnetic fields, approaching the subband spacing E_{01}, subband–Landau-level coupling takes place. The coupling leads to anti-crossing of the levels and this causes strong bending of the Landau levels, so the CR field is greatly modified. If we assume a parabolic quantum well, we can readily show that $B(\theta)$ follows the $1/\cos\theta$ law when the ratio of $\overline{h}\omega_c$ to the subband spacing E_{01} is very small, but as the ratio $\overline{h}\omega_c/E_{01}$ increases, $B(\theta)$ is enhanced to a higher field than that of the $1/\cos\theta$ law. When $\overline{h}\omega_c/E_{01}$ exceeds unity, $B(\theta)$ exhibits a dramatic decease and becomes lower than that of the $1/\cos\theta$ law. In order to investigate such angular dependence, we prepared various samples of GaAs/AlGaAs quantum

wells, with different well widths L_w, Al concentrations x, barrier heights E_{bar}, and carrier concentrations n.

Figure 7 shows the angular dependence of the CR trace for sample 2 ($E_{bar} = 165$ meV, $L_w = 10$ nm, $n = 2.75 \times 10^{11}$ cm^{-2}) [17]. At a wavelength of 16.9 μm, $B(\theta)$ increases with increasing θ, but the angular dependence is stronger than the $1/\cos\theta$ law. This is reasonable if we consider the value $\hbar\omega_c/E_{01} \sim 0.7$. At 9.55 μm, however, $B(\theta)$ decreases with increasing θ. This result can also be explained on the basis of the value $\hbar\omega_c/E_{01} \sim 1.3$. It should be noted that the traces obtained with rising and falling magnetic field almost coincide and a clear spin splitting is observed.

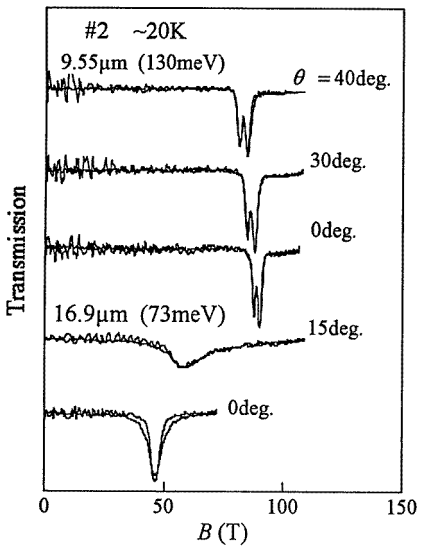

Figure 7. Cyclotron resonance traces for sample 2 at various tilt angles.

The angular dependence for sample 3 ($E_{bar} = 165$ meV, $L_w = 5$ nm, $n = 0.85 \times 10^{11}$ cm^{-2}) which has a smaller value of L_w is shown in figure 8. It should be noted that $B(\theta)$ increases with increasing θ for $\lambda = 16.9$ μm, whilst for $\lambda = 10.6$ μm, $B(\theta)$ is almost independent of θ and the absorption intensity is a strongly decreasing function of θ. In this sample, the first excited subband is beyond the barrier. The intensity decrease can be explained by the fact that while the first excited Landau level ($N = 1$) is still inside the well for $\lambda = 16.9$ μm, it exceeds the barrier height ($\hbar\omega_c > E_{bar}$) for $\lambda = 10.6$ μm. In the latter case, the $N = 1$ Landau level of the confined first subband is strongly coupled with the unconfined Landau level belonging to the subbands in the continuum in the tilted magnetic fields. The intensity thus decreases as the wave-function of the excited state extends to the barrier layer.

Figure 9 shows the CR spectra for sample 6 ($E_{bar} = 330$ meV, $L_w = 10$ nm, $n = 1.3 \times 10^{11}$ cm^{-2}). As the measurement was performed using the single-turn coil technique, two traces are obtained with one shot of the pulsed field. The field rises and falls in 7 μs. At $\lambda = 16.9$ μm, the traces with the rising field (up-sweep) and falling field (down-sweep) coincide with each other. At $\lambda = 10.6$ μm, however, a very large hysteresis is observed between the up-trace and the down-trace. The hysteresis is observed only when the photon energy is close to the E_{10}. By comparing the traces for various angles, we found that the down-sweeps give the right traces in equilibrium, whilst the up-sweeps take various non-equilibrium profiles depending on the sweep speed. The hysteresis is nothing to do with artefacts due to

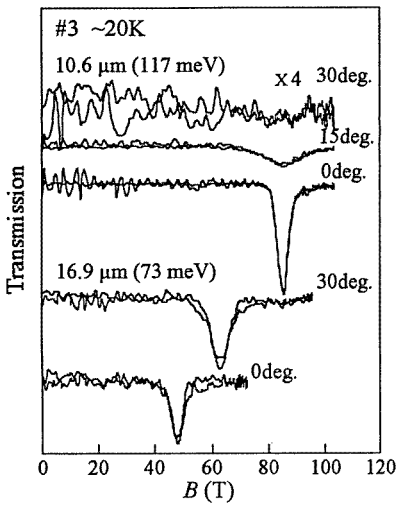

Figure 8. Cyclotron resonance traces for sample 3 at various tilt angles. The first excited subband is beyond the barrier. The $N = 1$ Landau level is above the barrier height for $\lambda = 10.6$ μm.

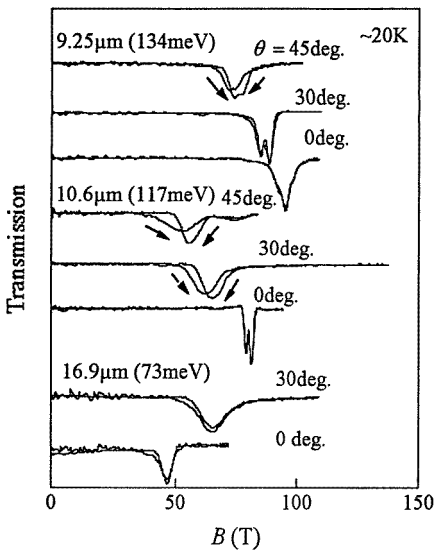

Figure 9. Cyclotron resonance traces for sample 6 at various tilt angles.

the response time of the detectors, etc, as there is no such hysteresis for certain angles. It is not due to the saturation of the excited states either, because we did not observe any light intensity dependence of the hysteresis. The origin of the hysteresis is not known at present, but it is ascribed to some kind of relaxation phenomenon of the electrons in the ground state or the formation of coupled states [17].

4. Conclusion

In conclusion, we have measured magneto-optical spectra for various systems of quantum wells, short-period superlattices, quantum wires, and quantum dots under very high magnetic fields. In the magneto-photoluminescence and magneto-absorption experiments, we observed characteristic features of low-dimensional excitons in high magnetic fields. In the cyclotron resonance experiments with the magnetic field tilted away from the growth direction, we found new features originating from the subband–Landau-level coupling.

Acknowledgments

The authors are obliged to our co-workers, Professor Y Shiraki, Dr F Isshiki, Dr N Usami, Professor H Nakashima, Dr Y Sakuma, Dr Y Awano, Dr T Futatsugi, Dr N Yokoyama, Dr H Saku and Dr Y Hirayama for providing the samples used in the present work.

References

[1] Miura N 1994 *Physica* B **201** 40
[2] Tarucha S, Okamoto H, Iwasa Y and Miura N 1984 *Solid State Commun.* **52** 815
[3] Green R L and Bajaj K K 1988 *Solid State Commun.* **45** 831
[4] Yafet Y, Keyes R W and Adams E N 1956 *J. Phys. Chem. Solids* **1** 137
[5] Iwasa Y, Miura N, Tarucha S, Okamoto H and Ando T 1986 *Surf. Sci.* **170** 587
[6] Uchida K, Miura N, Kitamura J and Kukimoto H 1996 *Phys. Rev.* B **53** 4809
[7] Issiki F, Fukatsu S, Ohta T and Shiraki Y 1996 *Solid-State Electron.* **40** 43
[8] Uchida K, Miura N, Sugita T, Issiki F, Usami N and Shiraki Y 1998 *Physica* B **249–251** 909
[9] Nagamune Y, Arakawa Y, Tsukamoto S, Nishioka M, Sasaki S and Miura N 1992 *Phys. Rev. Lett.* **69** 2963
[10] Takeuchi M, Shiba K, Sato K, Huang H K, Inoue K and Nakashima H 1995 *Japan. J. Appl. Phys.* **34** 4411
[11] Wang P D, Merz J L, Fafard S, Leon R, Leonard D, Medeiros-Ribeiro G, Oestreich M, Petroff P M, Uchida K, Miura N, Akiyama H and Sakaki H 1996 *Phys. Rev.* B **53** 16 458
[12] Samuelson L, Anand S, Carlsson N, Castrillo P, Georgsson K, Hessman D, Pistol M-E, Pryor C, Seifert W, Wallenberg L R, Carlsson A, Bovin J-O, Nomura S, Aoyagi Y, Sugano T, Uchida K and Miura N 1996 *Proc. 23rd Int. Conf. on Physics of Semiconductors* ed M Scheffler and R Zimmermann (Singapore: World Scientific) p 1269
[13] Hayden R K, Uchida K, Miura N, Plicmeni A, Stoddart S T, Henini M, Eaves L, Carmona H A, Moriarty P, Beton P H, Main P C, Fromhold T M and Sheard F W 1998 *Physica* B **249–251** 262
[14] Rinaldi R, Cingolani R, Lipsanen H, Sopanen M, Tuikki J, Brasken M, Ahopelto J, Uchida K, Miura N and Arakawa Y 1999 *Proc. 24th Int. Conf. Physics of Semiconductors (Jerusalem, 1999)* (Singapore: World Scientific)
[15] Sugiyama Y, Sakuma Y, Muto S and Yokoyama N 1995 *Appl. Phys. Lett.* **67** 256
[16] Uchida K, Miura N, Sakuma Y, Awano Y, Futatsugi T and Yokoyama N 1998 *Physica* B **249–251** 247
[17] Arimoto H, Saku T, Hirayama Y and Miura N 1998 *Physica* B **256–258** 343